Enhancing Induction Motor Reliability Through Advanced Feature Selection and Diagnostic Models in Low-Load Conditions

Chibuzo Nwabufo Okwuosa, Jang-Wook Hur*
Department of Mechanical Engineering (Department of Aeronautics, Mechanical and Electronic Convergence Engineering)
Kumoh National Institute of Technology,
61 Daehak-ro, Gumi-si 39177, Gyeonsangbuk-do, Republic of Korea
okwuosachibuzo3@kumoh.ac.kr, hhjw88@kumoh.ac.kr*

***Abstract*—In induction motors, stator windings are critical for optimal magnetic field distribution, influencing rotor bar induction and motor performance. Motor component failure is undesirable and often necessitates system overhauls. This paper presents a comparative analysis of feature selection techniques filter-based, wrapper-based, and embedded methodsfor diagnosing stator winding faults in squirrel cage induction motors and selecting a reliable cost-efficient feature selection technique with high efficiency. These techniques are applied using varying motor current data signals under low-load conditions. By leveraging advanced signal processing tools, the study demonstrated that the embedded techniques presented a superior computational efficiency and diagnostic model than the other techniques using the XGboost classifier algorithm. Preliminary results highlight the potential of these techniques to improve fault detection while addressing challenges such as noise and signal complexity. Future research will explore the integration of Explainable AI (XAI) to enhance transparency and trust in diagnostic models.**

***Index Terms*—Fault diagnosis, Filter-based feature selection, Peak detection, Hilbert transform, Signal processing, Forward Selection, Feature Importance.**

I. Introduction

INDUCTION motors (IMs) are essential in a wide range of applications, from large industrial machinery to domestic appliances, due to their dependability, relatively inexpensive maintenance, adaptability, and robustness [1]. However, their performance can be significantly impacted by stator winding faults, which account for a majority of failures in squirrel cage induction motors (SCIMs). Condition-based monitoring (CBM) techniques, such as Motor Current Signature Analysis (MCSA), offer promising non-invasive diagnostic capabilities but face challenges related to noise and signal complexity, especially under low-load conditions.

This work was partly supported by Innovative Human Resource Development for Local Intellectualization program through the Institute of Information & Communications Technology Planning & Evaluation(IITP) grant funded by the Korea government(MSIT) (IITP-2024-2020-0-01612, 50%) and grant funded by the MSIT(Ministry of Science and ICT), Korea, under the ITRC(Information Technology Research Center) support program(IITP-2024-RS-2024-00438430, 50%) supervised by the IITP(Institute for Information & Communications Technology Planning & Evaluation) .

Induction motors are critical in manufacturing but frequently experience breakdowns, with stator winding and bearing failures accounting for over 70% of errors in squirrel-cage induction motors [2]. Stator winding issues can lead to system-wide failures [3], while faults like turn-to-turn winding, though less severe, still require early detection. Traditionally, Motor Vibration Signature Analysis (MVSA) has been employed for Condition-Based Monitoring (CBM), as it utilizes vibration signals from machinery. However, these signals often contain noise, requiring extensive processing tools for noise elimination [4]. Alternatively, Motor Current Signature Analysis (MCSA) provides a less intrusive approach, offering information on mechanical conditions without physical interaction, which presents an efficient CBM methodology [5].

Signal processing is essential for optimizing CBM models. The Fast Fourier Transform (FFT) is a widely used technique in MCSA, revealing signal frequencies when time-domain data is insufficient. However, FFT struggles under low-load conditions or with stationary signals [6]–[8]. Consequently, advanced techniques such as the discrete wavelet transform (DWT), the Hilbert Huang transform (HHT), the wavelet transform (WT), and the Hilbert transform (HT) are often used to enhance performance. HT, in particular, is versatile and introduces phase shifts to signals, improving discrimination without altering their domain [8].FFT inefficiencies under low-load and stationary signals have led to efforts to address these limitations. For example, researchers in [9] combined FFT with supplementary methods like auto-correlation and peak detection to improve its performance. Their study measured power spectral density using FFT, but even with enhancements, the models accuracy remained inadequate, highlighting FFT's limitations in these conditions.

The classification model's efficiency heavily depends on feature preprocessing and engineering techniques. Methods like statistical analysis, linear discriminant analysis (LDA), independent component analysis (ICA), and principal component analysis (PCA) are commonly used for extracting and selecting relevant features [10]–[12]. Feature selection techniques such as filter-based feature selection (FFS), wrapper-

based feature selection (WFS), and embedded feature selection (EFS) help reduce model complexity, select relevant features, and minimize redundancy [13]–[15]. An in-depth study in [16] explored feature selection in big data analysis, underscoring its importance.

Several studies highlight the significance of feature selection. In [17], a correlation-based FFS technique was used, applying a 70% threshold to iteratively remove redundant features. The selected features, when trained with a support vector classifier, showed optimal performance. Similarly, Kumar et al. in [18] used an FFS relief algorithm to identify six critical features from a pool of 38 to detect misaligned rotor bar failure. These features were combined using machine learning algorithms to develop a health indicator, enabling both fault identification and severity measurement. These studies emphasize the role of feature selection in enhancing fault diagnostics and classification.

Consequently, this study presents a comparative analysis of filter-based correlation, feature importance, and wrapper-based feature selection techniques for diagnostic classifier models, with a focus on their application in identifying stator winding failures under low load conditions. Although previous research has generally favored WFS methods, due to their efficiency, it also notes their substantial computational demands. FFS approaches, on the other hand, are algorithm-independent for feature selection and require less computational cost [16], [19]. Although some research studies have presented comparative analysis between these feature selection techniques, none has been done in the context of SCIM at low load conditions. Hence, this research aims to identify the most suitable feature selection technique for diagnosing and classifying stator winding failures in squirrel cage induction motors under low-load conditions, using the most compatible classifier algorithm.

II. Experimental Setup and Failure Simulation

A. Experimental Setup

A 3-phase squirrel cage induction motor (SCIM) operates on electromagnetic induction principles, with stator windings inducing rotor motion. An abrupt stator fault can cause increased power consumption, unbalanced flux, insufficient rotor spinning, and overheating, threatening fire risk. A test bench (Figure 1a) was established to analyze motor behavior and fault effects under controlled experimental conditions.

To simulate a load instance, a brake effect was created by applying a 31.0-volt DC supply to the stator winding of the driven motor in a 3-phase SCIM setup. This induced a minor load on the driver motor, connected via a coupler (Figure 1a). Our data acquisition system employed a NI-9246 Current Module, with Current signal data acquired from the motor via current sensors connected to a 3-phase power supply and a CPU through the NI-9174 DAQ module. LabVIEW software converts these signals into numerical data for efficient Fault Detection and Isolation, enabling signal processing (see Figure 1b).

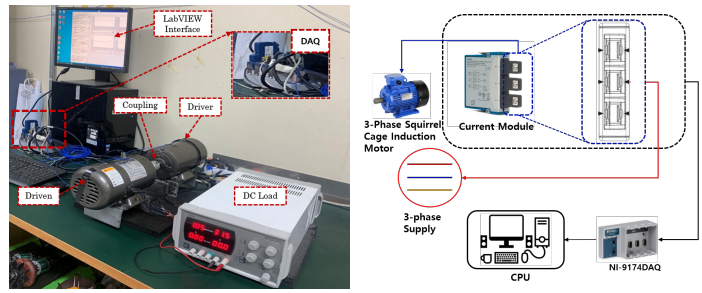

(a) (b)

Fig. 1. Experimental Setup and Data Collection: (**a**) Experimental-bench, (**b**) Data Acquisition Blueprint.

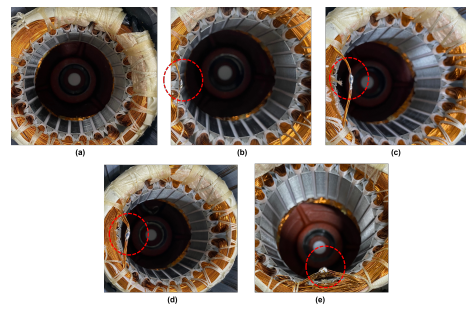

Fig. 2. **(a)** Healthy Condition. **(b)** Two turn windings of a phase. **(c)** Four turn windings of phase. **(d)** Six turn windings of a phase. **(e)** Eight turn windings of a phase.

B. Failure Simulation for Data Curation and Visualization

The study's objective is to identify the best model for feature selection techniques that can accurately classify various turn-to-turn short circuit failures under low-load conditions. To achieve this, it is crucial to collect sufficient data from these systems under various fault conditions. Faults ranging from two winding-turns bridged to eight winding-turns bridged are induced by manually removing the insulation coating to expose the current-carrying coils of the SCIM phases, creating the required failure instances for an efficient FDI process.

TABLE I
Operating Conditions

Condition Code	Definition
HTY-1	The healthy operational condition of the SCIM
SWF-2	Failure induced by linking two turn windings of a given phase
SWF-4	Failure induced by linking four turn windings of a given phase
SWF-6	Failure induced by linking six turn windings of a given phase
SWF-8	Failure induced by linking eight turn windings of a given phase

Five conditions, as summarized in Table I, were employed in the study: four induced fault conditions and one representing the healthy condition of the motor. These conditions form the datasets for the study.

III. Fault Diagnostic Methodology of SCIM

A. Proposed fault diagnostic model

The flowchart for the proposed fault diagnostic model is shown in Figure 3. Current signals, spanning fault severity

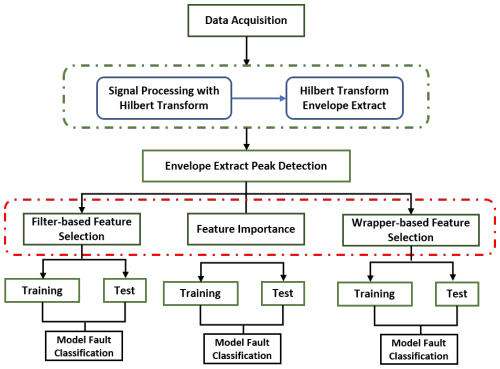

Fig. 3. The proposed system Model.

levels and a healthy stator, undergo Hilbert transform for signal pre-processing. Furthermore, a peak detection algorithm is implemented on the magnitude envelope to extract the peak signals. These peak extracts are statistically pre-processed to extract more robust features. The study's goal is to determine the ideal feature selection technique by thoroughly comparing the FFS, WFS, a Embedded methods. These techniques are employed to uniquely select discriminant features for efficient fault classification from the extracted peak features, and their performances are evaluated using global evaluation metrics to determine the most suitable technique.

B. Signal processing with Hilbert Transform

In practice, the bulk of signals have non-stationary behavior. Signals that exhibit minor variations over a particular period are called stationary. However, fault signals under low-load motor conditions and non-stationary require robust signal processing approaches [7], [18].

HT is an efficient time-domain signal analytical technique that operates by infusing a $\pm\pi/2$ phase shift in the original signal while maintaining the signal's domain. This shift separates the analytic signal from the original signal, which is a distinguishing feature of HT. Maintaining the original signal's domain post-transformation stands out as one of HT's essential characteristics; this creates an orthogonality between the analytic and original signals [20], [21]. Defining HT as the signal's convolution using $(\frac{1}{\pi t})$ emphasizes the signal's local characteristics and highlights its features.

Nevertheless, the function of HT $(\frac{1}{\pi t})$ is not always integrable, which prevents the integral on which the convolutional process is based from converging. Therefore, The general definition of the HT using the Cauchy principle value is presented in Equation 1:

$$H(x(t)) = \frac{1}{\pi} PV \int_{-\infty}^{\infty} \frac{x(\tau)}{(t-\tau)} d\tau = \frac{1}{\pi} PV \int_{-\infty}^{\infty} \frac{x(t-\tau)}{\tau} d\tau \tag{1}$$

PV stands for the singular integral principle of Cauchy. Due to the restrictions imposed by the non-integrable HT function, the Cauchy singular integral value is usually utilized as HT's initial definition. Its resultant analytical signal is thus; made up of both real and imaginary signals as a result of the non-intergable function.

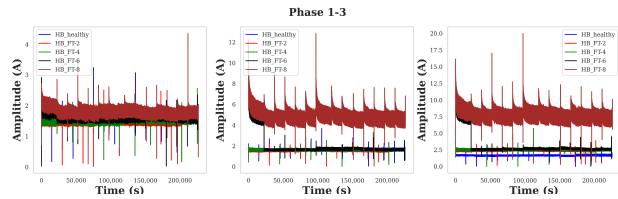

Fig. 4. Signal Magnitude Envelope Transform Pictorial Overview.

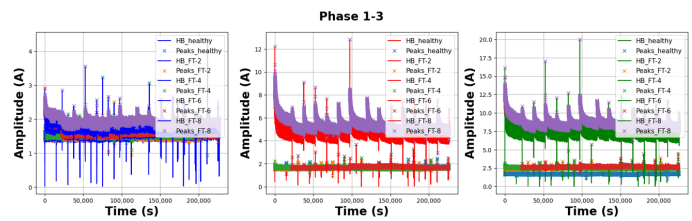

Fig. 5. Signal Magnitude Envelope Transform Peak Detection Overview.

Nonetheless, the magnitude envelope technique was introduced in this study to extract relevant insights from the analytical data while minimizing its inherent complexity. This approach serves two purposes: it reduces the influence of low-energy components while amplifying critical information and high-energy components within the analytical signal. The magnitude envelope can be mathematically represented as follows:

$$\text{Magnitude envelope } = |HT|^2 \tag{2}$$

Figure 4 depicts the magnitude envelope analysis of all motor current operating signals under low-load conditions. The modulating amplitudes for each operating condition demonstrate the magnitude envelope technique's efficiency in accentuating relevant qualities while suppressing less significant elements. This suggests that the modified signals may contain the discriminative information necessary for a reliable FDI framework implementation.

C. Magnitude Envelope Peak Detection Feature Extraction

The research employed a peak detection feature extraction technique which is a technique that identifies the locations and values of significant peaks and/or local maxima in a signal. In this study, a peak detection algorithm is implemented on the Hilbert magnitude envelope of the raw signal as our feature extraction methodology. This technique is initiated with the aim of extracting the discriminative feature for the various operating conditions at low-load conditions.

For a discrete signal $Y[x]$, if y represents the index signal, then $Y[x]$ can be considered its peak in satisfies the following conditions:

$$Y[x] > Y[x-1] \text{ and } Y[x] > Y[x+1]$$

This condition, when satisfied by a given signal, indicates that its value at index x is greater than its nearest neighbors, making $Y[x]$ a peak and/or local minima.

However, in the context of this study, to effectively implement the peak detection algorithm on the Hilbert magnitude envelope, the Hilbert magnitude transform $E[x]$ of a signal $Y[x]$ is first derived, and then the peaks are detected using the formula below:

$$\text{Peak at } x \text{ if } E[x] > E[x-1] \text{ and } E[x] > E[x+1] \quad (3)$$

Where $E[x-1]$ and $E[x+1]$ are the Hilbert magnitude envelope peak values at the neighboring time points.

This peak detection technique aims to extract meaningful details about the system's behavior under various operating conditions presented in our study. To further amplify the extracted features, 30 features are statistically extracted from each operating condition using a window-step statistical technique. This approach involves employing a window frame that divides the extracted peaks of each operating condition into 30 feature columns.

Additionally, these extracted features are standardized to ensure adaptability and improve performance when fed into ML classifier algorithms. Standardization centers on data scaling based on standard deviation, which, in this case, helps emphasize the extracted peaks of the operating conditions, amplifying discriminative characteristics. Furthermore, the impact of outliers, which might represent noise rather than fault characteristics, can be effectively suppressed via standardization, thereby increasing the discriminative strength of the features.

D. Feature Selection Techniques

1) Pearson correlation filter-based selection: In this study, the subset of the Filter method employed is the Pearson correlation feature selection (PCFS) technique. Its basic operational technique involves a metric evaluation of the linear relationship and similarity between two datasets, with its evaluation values ranging from -1 for negative correlation to +1 for positive correlation [11], [17]. Its selection and filtering are solely dependent on the similarity of features, hence, it is assumed to be feasible to select discriminative features.

A mathematical representation of PC is shown below [17]:

$$r = \frac{\text{cov}(Y,Z)}{\sigma_Y \sigma_Z} = \frac{\frac{\sum_{i=1}^{n}(y_i-\bar{y})(z_i-\bar{z})}{n-1}}{\sqrt{\frac{\sum_{i=1}^{n}(y_i-\bar{y})^2}{n-1}}\sqrt{\frac{\sum_{i=1}^{n}(z_i-\bar{z})^2}{n-1}}} \quad (4)$$

To ensure a thorough analysis, 6 filter feature cases (8,12,16,19,22,25) were generated using the PCFS. This was achieved by implementing the algorithm to filter a given percentage of similarity until these desired varieties of features were successfully selected from the 30 features. Figure 6 shows the correlation plot of all the six filtered feature feature cases using PCFS.

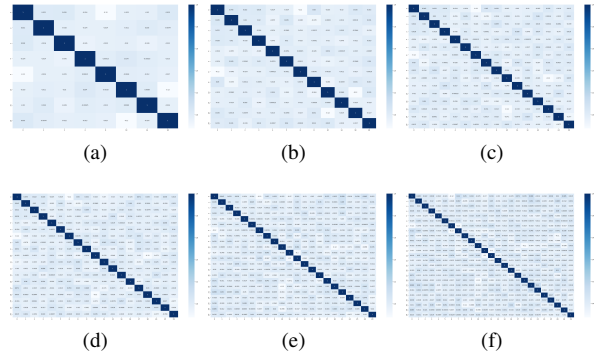

Fig. 6. Pearson Correlation Feature Selection Plot: (**a**) Eight Features, (**b**) Twelve Features (**c**) Sixteen Features (**d**) Nineteen Features (**e**) Twenty-Two Features (**f**) Twenty-Five Features.

2) Forward Selection: In this study, the forward selection (FS) subset of the wrapper feature selection methodology is utilized. This is because it is one of the fastest wrapper feature selection techniques. The pseudocode of the wrapper-based feature selection process is shown in algorithm 1.

Algorithm 1 A pseudo code of the Forward Wrapper-based process

```
Input: X = {x_1, x_2, ..., x_n}
Output: Y_s = {y_k | k = 1, 2, ..., s; y_k ∈ X}
where s = (0, 1, 2, ..., n)
m = The specified number of desired features
Initialization: Y_0 = ∅, s = 0
Steps:
while s < m do
   y^+ = arg max K(Y_s + y), where y ∈ (X − Y_s)
   where y^+ = best feature per iteration
    update Y_{s+1} = Y_s + y^+
    update s = s + 1
end while
end process
```

3) Feature Importance: XGBoost provides feature importance metrics using tree-based techniques classified as the Embedding feature selection method. The default technique, "Weight" (or Frequency), determines how frequently a feature is used to partition data across all trees in the model. Other methods include "Gain," which utilizes a feature's average gain (typically the most accurate), and "Cover," which computes the average coverage of data points affected by a feature. XGBoost uses the F-score to analyze feature performance. In this study, the Frequency technique was adopted for feature selection since it was more appropriate for the dataset.

IV. Results and Evaluations

A. Comparative evaluation

This section discusses the performance of 10 ML classification models using the 3 feature selection techniques. Figure 8 provides an analytical overview of the results. Accuracy improved across all models as the number of features increased, particularly for features selected using the PCFS technique. In the first section of the analysis, the accuracy and the computational cost of the models are used as the primary evaluation metrics. However, models using features selected by PCFS

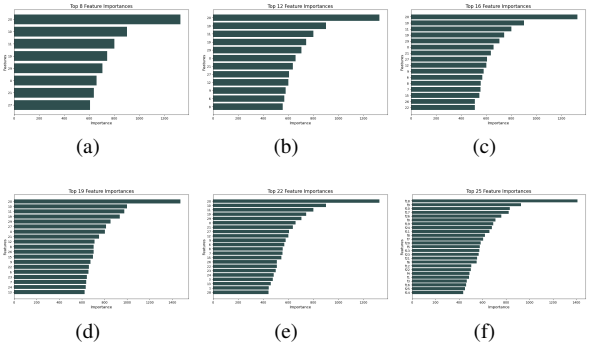

Fig. 7. Pearson Correlation Feature Selection Plot: (**a**) Eight Features, (**b**) Twelve Features (**c**) Sixteen Features (**d**) Nineteen Features (**e**) Twenty-Two Features (**f**) Twenty-Five Features.

TABLE II
ARCHITECTURAL PARAMETERS OF THE CLASSIFIER MODELS.

Model	Model Parameter	Model Parameter Value
SVM	Kernel, Regularizer (C), gamma (γ)	RBF, C =1 , γ = scale
SVM_l	Kernel, Regularizer (C), gamma (γ)	Linear, C =1 , γ = scale
$K-NN$	k	5
SGD	Random-state, loss-function	101, modified Huber
RF	n estimators, random-state	70, 101
DT	Criterion, Maximum depth	Entropy, 5
NB	Default	Default
ABC	n estimators, learning rate	Default
XGB	—	Default
GBC	n estimators	Default

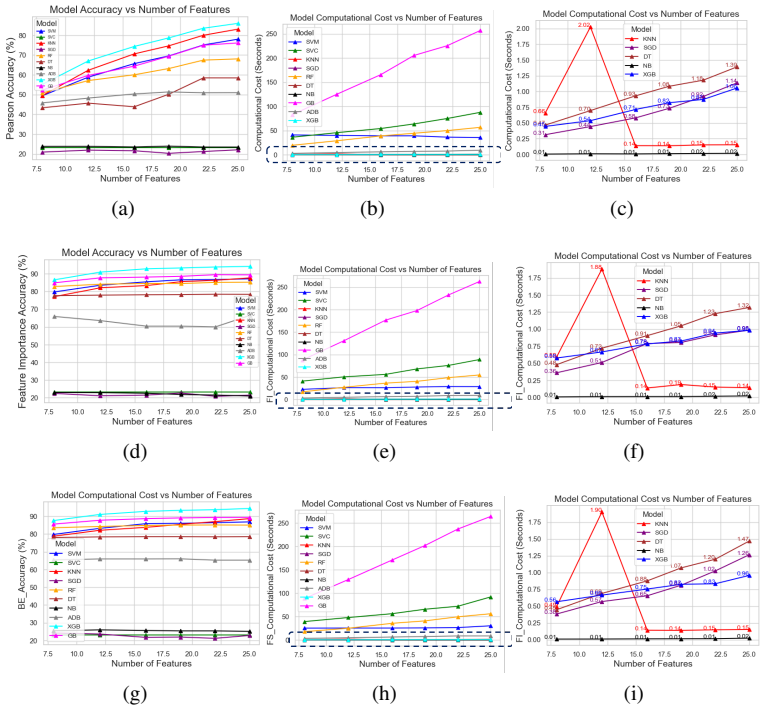

Fig. 8. Metrics Evaluation of the Models: (**a**) Pearson Accuracy (**b**) Pearson Computational Cost (**c**) Zoomed in Pearson Computational Cost (**d**) Feature Importance Accuracy (**e**) Feature Importance Computational Cost (**f**) Zoomed in Feature Importance Computational Cost (**g**) Forward Selection Accuracy (**h**) Forward Selection Computational Cost (**f**) Zoomed in Forward Selection Computational Cost.

exhibited the lowest overall performance. In contrast, features selected through FI and FS showed only minor differences in accuracy, which are further analyzed. Computational costs across the three techniques were comparable as shown in 8, but the higher accuracy and efficiency of models using FI and FS made them standout approaches for this study.

The dataset comprised 35,528 rows and 30 columns, representing various operating conditions, and was split 80% for training and 20% for testing. The training was conducted on an 11th Gen Intel(R) Core i7-11700 processor with 32GB of RAM. Data were generated from systems with induced faults to simulate real-world scenarios, emphasizing low-load conditions where signal quality is challenging. The poor performance of PCFS highlights the limitations of correlation-based feature selection, which operates independently of models, sometimes retaining redundant features that do not enhance classification.

FS and FI-based features consistently outperformed PCFS due to their model-dependent nature.FS allows iterative feature selection across multiple classifiers, offering greater flexibility, while FI evaluates features based on their importance within a specific model. Upon deeper assessment, the performance of ADB and NB with both FS and FI features, as shown in Figure 8, highlights a case where the slight differences between these two highly efficient feature selection tools can be addressed. In Figure 8d, the accuracy of ADB (65.4095%) showed a drop after the first instance (training with 8 features), which was not the case with FS features, as shown in Figure 8g. Additionally, in Figures 8d and 8g, the difference in accuracy is evident, with FS features showing slightly better performance. This discrepancy could be attributed to the nature of the Feature Importance (FI) technique, which selects features using a limited machine learning algorithm for feature selection. This may result in features that do not adapt adequately to other ML classifiers during model training. Contrarily, FS, a wrapper-based feature selection method, provides greater flexibility by allowing different machine learning algorithms to be used for both feature selection and model training.

To further analyze the models' performances, the confusion matrix for the XGB model's performance with both FI and FS (the best-performing models, achieving accuracies of 94.188% and 94.413%, respectively) is presented. A confusion matrix provides details on the true positives, false positives, true negatives, and false negatives of a model, offering insights into its performance across each class. As shown in Figure 9, the models performed exceptionally well across all classes. However, the complexity of the data signals was evident, with most false positives concentrated around HTY-1, SWF-2, and SWF-4. This is likely because, at low-load instances, fault signatures in induction motors are less pronounced, particularly for less critical faults such as SWF-2 and SWF-4.

Furthermore, the computational cost of the feature selection process for each technique must be considered to ensure a thorough analytical comparison of the three feature selection methods. Table III summarizes the computational cost of XGB with each feature selection technique. The computational cost

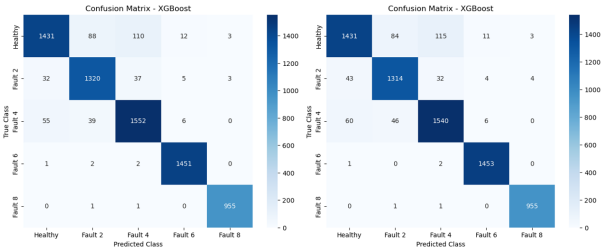

(a) (b)

Fig. 9. Confusion Matrix: (**a**) XGB FI (**b**) XGB FS.

TABLE III
FEATURE SELECTION COMPUTATIONAL COST FOR FI AND FS.

Feature No	FI Cost (Secs)	FS Cost (Secs)
8	0.001995	78
12	0.001995	145
16	0.001995	205
19	0.001995	244
22	0.001995	289
25	0.001995	320

of FI remained constant across varying feature numbers, while FS showed a significant increase, from 78 to 320 seconds. This highlights the high computational demand of the wrapper-based feature selection process. This suggests that embedded methods, with their efficient and cost-effective computational performance, present a better option compared to wrapper and filter-based feature selection techniques.

V. CONCLUSION AND FUTURE WORKS

This research provides a comparative analysis of filter-based, embedded, and wrapper-based methods for fault classification in SCIM under low-load conditions. The model results showed that embedded and wrapper-based methods selected better model adaptive features, achieving better test accuracies. However, embedded methods offered similar performance to wrapper-based methods while being more computationally efficient making it the optimal option. Future work will incorporate Explainable AI (XAI) to enhance model transparency by providing interpretable model decisions, enabling broader trust and understanding. Additionally, digital twin technology will be explored to create virtual replicas of induction motors for real-time monitoring and fault prediction, bridging the gap between theoretical research and industrial applications.

REFERENCES

[1] A. Choudhary, R. K. Mishra, S. Fatima, B. K. Panigrahi, "Multi-input CNN based vibro-acoustic fusion for accurate fault diagnosis of induction motor," in *Eng. Appl. Artif. Intell.,* vol. 120, 2023, pp. 105872, doi.org/10.1016/j.engappai.2023.105872.

[2] R. Jaros, R. Byrtus, J. Dohnal, J. Koziorek, P. Zmij, R. Martnek, "Advanced Signal Processing Methods for Condition Monitoring," in *Archives of Computational Methods in Engineering,* vol. 30, 2022, pp. 1553-1577, doi.org/10.1007/s11831-022-09834-4.

[3] X. Liang, M. Z. Ali, H. Zhang, "Induction Motors Fault Diagnosis Using Finite Element Method: A Review," in *IEEE Transactions on Industry Applications,* vol. 56, April 2020, pp. 1205-1217, doi.org/10.1109/TIA.2019.2958908.

[4] J.-H Lee, C. N. Okwuosa, J.-W. Hur, "Extruder Machine Gear Fault Detection Using Autoencoder LSTM via Sensor Fusion Approach," in *Inventions,* vol. 8, November 2023, pp. 140, doi.org/10.3390/inventions8060140

[5] J. Bonet-Jara, J. Pons-Llinares, "A Precise, General, Non-Invasive and Automatic Speed Estimation Method for MCSA Diagnosis and Efficiency Estimation of Induction Motors," in *IEEE Transactions on Energy Conversion,* vol. 38, June 2023, pp. 1257-1267, doi.org/10.1109/TEC.2022.3220853.

[6] X. Bessam, Ali, Z. Mohammad, H. Zhang, "Detection of broken rotor bar faults in induction motor at low load using neural network," in *ISA Trans,* vol. 64, September 2016, pp. 241246, doi.org/10.1016/j.isatra.2016.06.004.

[7] B. Konar, P. Chattopadhyay, "Multi-class fault diagnosis of induction motor using Hilbert and Wavelet Transform," in *Applied Soft Computing,* vol. 56, May 2015, pp. 341-352, doi.org/10.1016/j.asoc.2014.11.062.

[8] M. B. Abd-el-Malek, A. K. Abdelsalam, O. E. Zhang, " Novel approach using Hilbert Transform for multiple broken rotor bars fault location detection for three phase induction motor," in *IISA Transactions,* vol. 80, September 2018, pp. 439-457,

[9] C. N. Okwuosa, U. E. Akpudo, J.-W. Hur, "A Cost-Efficient MCSA-Based Fault Diagnostic Framework for SCIM at Low-Load Conditions," in *Algorithms,* vol. 15, May 2022, pp. 212, doi.org/10.3390/a15060212.

[10] N. K. Booker, P. Knights, J.D. Gates, R. E. Clegg, "Applying principal component analysis (PCA) to the selection of forensic analysis methodologies," in *Engineering Failure Analysis,* vol. 132, Aug 2022, pp. 105937, doi.org/10.1016/j.engfailanal.2021.105937.

[11] A. B. Kareem, J.-W. Hur, "Towards Data-Driven Fault Diagnostics Framework for SMPS-AEC Using Supervised Learning Algorithms," in *Electronics,* vol. 11, May 2022, pp. 2492, doi.org/10.3390/electronics11162492.

[12] Y. J. Yoo, "Fault Detection of Induction Motor Using Fast Fourier Transform with Feature Selection via Principal Component Analysis," in *Int. J. Precis. Eng. Manuf.,* vol. 20, June 2019, pp. 1543-1552, doi.org/10.1007/s12541-019-00176-z.

[13] S. Buchaiah, P. Shakya, "Bearing fault diagnosis and prognosis using data fusion based feature extraction and feature selection," in *Measurement,* vol. 188, Jan 2022, pp. 110506, doi.org/10.1016/j.measurement.2021.110506.

[14] M. Cherrington, F. Thabtah, J. Lu and Q. Xu, "Feature Selection: Filter Methods Performance Challenges," *International Conference on Computer and Information Sciences (ICCIS),* 2019, pp. 1-4, doi.org/10.1109/ICCISci.2019.8716478.

[15] M. S. Bonab, "A wrapper-based feature selection for improving performance of intrusion detection systems," *International Journal of Communication Systems* vol. 33, 2020, pp. , doi.org/10.1002/dac.4434.

[16] H.M. Abdulwahab, S. Ajitha, M.A.N. Saif " Feature selection techniques in the context of big data: taxonomy and analysis," *Appl Intell* 2022, pp. vol. 52, doi.org/10.1007/s10489-021-03118-3.

[17] C. N. Okwuosa, J.-W. Hur, " A Filter-Based Feature-Engineering-Assisted SVC Fault Classification for SCIM at Minor-Load Conditions," *Energies* 2022, pp. vol. 15, doi.org/10.3390/en15207597.

[18] A. Kumar, C. P. Gandhi, X. Liu, Y. Liu, Y. Zhou, R. Kumar, J. Xiang, "A novel health indicator developed using filter-based feature selection algorithm for the identification of rotor defects," *Proceedings of the Institution of Mechanical Engineers, Part O: Risk and Reliability* vol. 236, May 2022, pp. , doi.org/10.1177/1748006X20916953.

[19] N. D. Cilia, T. DAlessandro, C. De Stefano, F. Fontanella, A. Scotto di Freca, "Comparing filter and wrapper approaches for feature selection in handwritten character recognition," in *Pattern Recognition Letters,* vol. 168, April 2023, pp. 39-46, doi.org/10.1016/j.patrec.2023.02.028.

[20] C. N. Okwuosa and J. -W. Hur, "An Intelligent Hybrid Feature Selection Approach for SCIM Inter-Turn Fault Classification at Minor Load Conditions Using Supervised Learning," in *IEEE Access,* vol. 11, April 2023, pp. 89907-89920, doi: 10.1109/ACCESS.2023.3266865.

[21] M. Deeb, N. F. Kotelenets, V. B. Bal, T. Assaf and G. Ibrahim, "Envelope Stator Current Analysis of an Induction Motor for Short-Circuit Fault Diagnosis," in *2022 4th International Youth Conference on Radio Electronics, Electrical and Power Engineering (REEPE), Moscow, Russian Federation,* 2022, pp. 1-6, doi: 10.1109/REEPE53907.2022.9731369.